

# Quaternion-MUSIC for Vector-Sensor Array Processing

Sebastian Miron, Nicolas Le Bihan, and Jérôme I. Mars

**Abstract**—This paper considers the problem of direction of arrival (DOA) and polarization parameters estimation in the case of multiple polarized sources impinging on a vector-sensor array. The quaternion model is used, and a data covariance model is proposed using quaternion formalism. A comparison between long vector orthogonality and quaternion vector orthogonality is also performed, and its implications for signal subspace estimation are discussed. Consequently, a MUSIC-like algorithm is presented, allowing estimation of wave's DOAs and polarization parameters. The algorithm is tested in numerical simulations, and performance analysis is conducted. When compared with other MUSIC-like algorithms for vector-sensor array, the newly proposed algorithm results in a reduction by half of memory requirements for representation of data covariance model and reduces the computational effort, for equivalent performance. This paper also illustrates a compact and elegant way of dealing with multicomponent complex-valued data.

**Index Terms**—Polarization, Q-MUSIC, quaternion eigenvalue decomposition (QEVD), quaternion spectral matrix (QSM), quaternion vector orthogonality, vector-sensor array.

## I. INTRODUCTION

HAMILTON'S quaternions  $\mathbb{H}$ , as a nontrivial generalization of complex numbers  $\mathbb{C}$ , have been considered for a long time of pure theoretical interest. In signal processing, it is only in the last decade that quaternion-based algorithms were proposed [1]. More recently, hypercomplex spectral transformations and color images processing techniques have been introduced by Ell and Sangwine in [2]–[5] and Pei and Cheng in [6]. A hypercomplex version of the multidimensional complex signals [7] was also proposed by Bülow and Sommer [8]. In seismic data processing, as multicomponent acquisitions fit perfectly with the quaternion model, quaternion algebra has been used to extract seismic attributes [9], [10], to enhance signal-to-noise ratio (SNR) and to separate sources on multicomponent<sup>1</sup> seismic data set [11], [12]. Most of these methods encode a real-valued three-component signal on the three imaginary parts of a pure quaternion (see Subsection II-A). In this paper, we propose a data model allowing to deal with multicomponent modulus-phase information by means of quaternions. The resulting data model is then used to illustrate an eigenstructure-based al-

gorithm for vector-sensor array processing yielding direction of arrival (DOA) and polarization parameters estimation.

Scalar-sensor array processing algorithms and the high-resolution methods for DOA estimation are well documented in the literature (see [13]–[16] and references therein). In the last decade, as vector-sensors became more and more reliable, polarization has been added to estimation process as an essential attribute to characterize sources, in addition to their DOAs. Consequently, multiple authors have proposed algorithms for multicomponent data processing. MUSIC-like methods for polarized arrays are presented in [17] and [18] and ESPRIT techniques in [19]–[21]. The Cramer–Rao bound for the vector-sensor case has been studied by Weiss and Friedlander in [22] and Nehorai and Paldi in [23]. A multilinear model for polarized seismic data and an eigenstructure-based algorithm (Vector-MUSIC) were also introduced in [24], yielding DOA and polarization parameters (intersensor amplitude ratio and intercomponent phase-shift) for sources impinging on a linear, uniform array. However, these approaches assume that the data are complex-valued, representing frequency domain samples of the recorded signals. Data covariance model is then defined as the set of second-order auto-moments and cross-moments between all components of all sensors. In this paper we propose a quaternion model for the multicomponent data that reduces by half the memory size required for data covariance model representation resulting in a increased rapidity of the algorithm (see Section V). Furthermore, we show that the orthogonality constraint imposed by the quaternion spectral matrix diagonalization is stronger than the one used for the classical spectral matrix (see Section III-B-2), and it provides a more accurate estimation of the signal subspace.

This paper is structured as follows. In Section II, a short description of quaternions is given and polarization model is introduced. Section III presents the quaternion spectral matrix (QSM) and discusses quaternion-valued vectors orthogonality. A description of the new Quaternion-MUSIC (Q-MUSIC) algorithm is given in Section IV, and its computational complexity is compared to long-vector algorithm complexity in Section V. The performances of Q-MUSIC algorithm evaluated in simulations are described in Section VI. Finally, Section VII presents the conclusions of this work.

## II. QUATERNION MODEL OF A POLARIZED SOURCE

### A. Quaternions

Quaternions are a four dimensional hypercomplex numbers system. Discovered by Hamilton in 1843 [25], they are an extension of complex numbers to four-dimensional (4-D) space.

Manuscript received November 8, 2004; revised May 3, 2005. The associate editor coordinating the review of this manuscript and approving it for publication was Dr. Jean Pierre Delmas.

The authors are with the Laboratoire des Images et des Signaux, 38 402 Saint Martin d'Hères Cedex, France (e-mail: sebastian.miron@lis.inpg.fr; nicolas.le-bihan@lis.inpg.fr; jerome.mars@lis.inpg.fr).

Digital Object Identifier 10.1109/TSP.2006.870630

<sup>1</sup>In this paper, the terms *multicomponent* data and *polarized* data are used to designate the data set recorded on a vector-sensor array.

A quaternion  $q$  is described by four components (one real and three imaginaries). It can be expressed in its Cartesian form as

$$q = a + ib + jc + kd \quad (1)$$

where

$$\begin{aligned} i^2 = j^2 = k^2 = ijk = -1 \\ ij = k \quad ji = -k \\ ki = j \quad ik = -j \\ jk = i \quad kj = -i. \end{aligned}$$

Many books discuss about quaternions and their properties. Basics about hypercomplex numbers systems can be found in [26], while a thorough review about quaternions can be found in Ward's book [27].

Several properties of complex numbers can be extended to quaternions. Some of them are as follows:

- the conjugate of  $q$ , noted  $\bar{q}$ , is given by  $\bar{q} = a - ib - jc - kd$ ;
- a *pure* quaternion is a quaternion which real part is null:  $q = ib + jc + kd$ ;
- the modulus of a quaternion  $q$  is  $|q| = \sqrt{q\bar{q}} = \sqrt{\bar{q}q} = \sqrt{a^2 + b^2 + c^2 + d^2}$  and its inverse is given by

$$q^{-1} = \frac{\bar{q}}{|q|^2} \quad (2)$$

- a quaternion is said to be *null* iff  $a = b = c = d = 0$ ;
- the set of quaternions, denoted by  $\mathbb{H}$ , forms a noncommutative normed division algebra, that means that given two quaternions  $q_1$  and  $q_2$

$$q_1 q_2 \neq q_2 q_1 \quad (3)$$

- conjugation over  $\mathbb{H}$  is an anti-involution

$$\overline{\overline{q_1} q_2} = \overline{q_2} \overline{q_1}. \quad (4)$$

It is well known [28] that a quaternion is uniquely expressed as:  $q = q^{(1)} + jq^{(2)}$ , where  $q^{(1)} = a + ib$  and  $q^{(2)} = c - id$ . This is known as the Cayley–Dickson form. It is also possible to express  $q$  in an alternate Cayley–Dickson form. Thus, any quaternion  $q$  can be written as

$$q = q' + iq'', \quad (5)$$

where  $q' = a + jc$  and  $q'' = b + jd$ . This notation will be used in the polarized signal quaternion model proposed in the following section.

### B. Polarization Model

Consider a scenario with one polarized source, assumed to be a centered, stationary stochastic process, emitting a wavefield in an isotropic, homogeneous medium. This wavefield is recorded on a two-component noise-free sensor, resulting in two highly correlated temporal series  $s_1[t_n], s_2[t_n] \in \mathbb{R}^{N_t}$ . After performing a discrete Fourier transform along time dimension

on each of the two components, the expression for the two components in frequency domain becomes

$$x_1[\nu_m] = \beta_1[\nu_m]e^{j\alpha_1[\nu_m]} \quad \text{and} \quad x_2[\nu_m] = \beta_2[\nu_m]e^{j\alpha_2[\nu_m]} \quad (6)$$

where  $x_1, x_2 \in \mathbb{C}^{N_\nu, \nu_m}$  is the discrete Fourier frequency,  $\beta_1, \beta_2$ , and  $\alpha_1, \alpha_2$  are the amplitudes and phases of the two components of the signal at the given frequency  $\nu_m$ .

Using the imaginary operator  $j$  instead of  $i$  as Fourier transformation axis, does not alter the physical meaning of Fourier phase and modulus. To simplify the notation, we shall ignore the frequency argument in these expressions and consider working at a given frequency  $\nu_m = \nu_{m_0}$ . As we do not have access to the exact amplitude and the initial phase of the source, the first component is considered as a reference and relative phase and amplitude are estimated. The statistical relationship between components can be expressed as a constant complex ratio between  $x_1$  and  $x_2$  or as a constant modulus ratio  $\beta_2/\beta_1 = \rho$  and a constant phase shift  $\varphi = \alpha_2 - \alpha_1$ . These two parameters  $\rho$  and  $\varphi$  must be estimated in order to describe the polarization ellipse orientation and eccentricity [29].

Using notations given in (6), we construct the quaternion signal  $x \in \mathbb{H}$ , describing a 2C signal on one sensor

$$x = \beta_1 e^{j\alpha_1} + i\beta_2 e^{j\alpha_2} \quad (7)$$

where

$$\begin{cases} e^{j\alpha_1} = \cos \alpha_1 + j \sin \alpha_1 \\ e^{j\alpha_2} = \cos \alpha_2 + j \sin \alpha_2 \end{cases}. \quad (8)$$

Expression (7) can be written in extended form as

$$x = \beta_1 \cos \alpha_1 + i\beta_2 \cos \alpha_2 + j\beta_1 \sin \alpha_1 + k\beta_2 \sin \alpha_2. \quad (9)$$

In this way, a new transformation is defined mapping the two-component complex-valued signal space to the quaternion-valued signal space. This transformation maps the even parts of the 2C signal on scalar and  $i$  imaginary fields of a quaternion while the odd parts are mapped to the two others remaining imaginary fields ( $j$  and  $k$ ).

Replacing  $\beta_2$  and  $\alpha_2$  in (7) by:

$$\begin{cases} \beta_2 = \rho\beta_1 \\ \alpha_2 = \varphi + \alpha_1 \end{cases} \quad (10)$$

observation  $x$  is written as the product between a quaternionic expression  $p(\rho, \varphi)$  describing the polarized wave behavior on the two components ( $\rho$  is the amplitude ratio and  $\varphi$  is the phase shift) and the complex amplitude of this wave on the first component

$$x = p(\rho, \varphi)\beta_1 e^{j\alpha_1} \quad (11)$$

where

$$p(\rho, \varphi) = 1 + i\rho e^{j\varphi}. \quad (12)$$

In order to extend this model to the multisensor case and to introduce the new Q-MUSIC algorithm, we consider a linear,

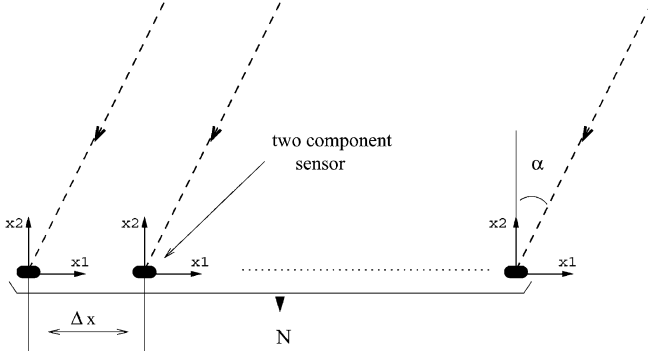


Fig. 1. Acquisition scheme.

uniform vector-sensor array of  $N$  sensors (Fig. 1). Assume that far-field waves from  $K$  sources ( $K$ -known,  $K < N$ ) impinge on this antenna. Sources are supposed to be decorrelated, spatially coherent and confined in the array plane. Their polarizations are also stationary in time and space (distance). Noise is spatially white and not polarized.<sup>2</sup>

To describe wavefield propagation along the array, it is necessary to model a time delay between sensors. In the far-field hypothesis, this delay is simply described as an intersensor phase shift  $\theta$ . The source DOA  $\alpha$  can then be calculated using the following formula:

$$\theta = 2\pi\nu \frac{\Delta x \sin \alpha}{v} \quad (13)$$

where  $\Delta x$  is the intersensors distance,  $v$  is the wave propagation velocity and  $\nu$  is the working frequency. Taking the first sensor (on the antenna) as reference,  $k$ th source propagation along the antenna is described by a vector  $\mathbf{a}_k \in \mathbb{C}^N$

$$\mathbf{a}_k(\theta_k) = [1, e^{-j\theta_k}, \dots, e^{-j(N-1)\theta_k}]^T. \quad (14)$$

Thus, the output of the vector-sensor array is given by a column quaternion vector  $\mathbf{x} \in \mathbb{H}^N$ , equal to the sum of the  $K$  sources contributions (added with a noise term)

$$\mathbf{x} = \sum_{k=1}^K \mathbf{d}_k \beta_{1k} \exp(j\alpha_{1k}) + \mathbf{n}. \quad (15)$$

In (15),  $\mathbf{n} \in \mathbb{H}^N$  contains noise contribution on all sensors and components,  $\beta_{1k}$  and  $\alpha_{1k}$  are given by (7) and  $\mathbf{d}_k \in \mathbb{H}^N$  is a quaternion vector describing  $k$ th source behavior on the vector-sensor array as

$$\mathbf{d}_k(\theta_k, \rho_k, \varphi_k) = p_k(\rho_k, \varphi_k) \mathbf{a}_k(\theta_k) \quad (16)$$

thus

$$\begin{aligned} \mathbf{d}_k(\theta_k, \rho_k, \varphi_k) &= [1 + i\rho_k e^{j\varphi_k}, e^{-j\theta_k} + i\rho_k e^{j(\varphi_k - \theta_k)}, \dots, \\ &e^{-j(N-1)\theta_k} + i\rho_k e^{j(\varphi_k - (N-1)\theta_k)}]^T. \end{aligned} \quad (17)$$

<sup>2</sup>Consider a two-component centered noise  $\mathbf{b}(m) = [b_1(m), b_2(m)]^T$  recorded on a single vector-sensor, where  $b_1(m), b_2(m)$  are Gaussian noise with variances  $\sigma_1, \sigma_2$ . Such a noise is *not polarized* if its covariance matrix  $\xi\{\mathbf{b}\mathbf{b}^H\} = \text{diag}(\sigma_1, \sigma_2)$ .

An unitary quaternion vector can be obtained dividing  $\mathbf{d}_k$  by its norm.<sup>3</sup> Thereafter,  $\mathbf{c}_k$  will refer to the unitary vector

$$\mathbf{c}_k = \frac{\mathbf{d}_k}{\|\mathbf{d}_k\|} \quad (18)$$

and  $\|\mathbf{d}_k\| = \sqrt{N(1 + \rho_k^2)}$  to its norm.

### III. QUATERNION SPECTRAL MATRIX

This section introduces a novel data covariance model for the polarization model presented in Section II.

#### A. Quaternion Spectral Matrix

For scalar-sensor arrays, the spectral matrix [30], [31] is given by the set of second order auto-moments and cross-moments of all sensors on the antenna. We introduce the equivalent second-order representation for a vector-sensor array using quaternion formalism. Quaternion spectral matrix (QSM)  $\Omega \in \mathbb{H}^{N \times N}$  is defined as

$$\Omega = \mathbb{E}\{\mathbf{x}\mathbf{x}^\triangleleft\} \quad (19)$$

where  $\mathbb{E}\{\cdot\}$  is the mathematical expectation operator and  $\mathbf{x} \in \mathbb{H}^N$  is the quaternionic observation vector introduced in (15). If we replace (15) in (19) and using relation (4),  $\Omega$  can be written as

$$\begin{aligned} \Omega &= \mathbb{E} \left\{ \left( \sum_{k=1}^K \mathbf{c}_k \|\mathbf{d}_k\| \beta_{1k} \exp(j\alpha_{1k}) + \mathbf{n} \right) \right. \\ &\quad \left. \times \left( \sum_{k=1}^K \mathbf{c}_k \|\mathbf{d}_k\| \beta_{1k} \exp(j\alpha_{1k}) + \mathbf{n} \right)^\triangleleft \right\} \\ &= \mathbb{E} \left\{ \left( \sum_{k=1}^K \mathbf{c}_k \|\mathbf{d}_k\| \beta_{1k} \exp(j\alpha_{1k}) + \mathbf{n} \right) \right. \\ &\quad \left. \times \left( \sum_{k=1}^K \beta_{1k} \exp(-j\alpha_{1k}) \mathbf{c}_k^\triangleleft \|\mathbf{d}_k\| + \mathbf{n}^\triangleleft \right) \right\}. \end{aligned} \quad (20)$$

Assuming the decorrelation between the noise and the sources and between sources themselves, the expression of the quaternion spectral matrix becomes

$$\Omega = \Omega_S + \Omega_N \quad (21)$$

where

$$\Omega_S = \sum_{k=1}^K \sigma_k^2 \mathbf{c}_k \mathbf{c}_k^\triangleleft \quad (22)$$

and  $\Omega_N = \mathbb{E}\{\mathbf{n}\mathbf{n}^\triangleleft\}$  is a matrix containing noise second-order statistics. In (21),  $\Omega_S$  is the signal part of QSM and  $\sigma_k^2 = (\beta_{1k} \|\mathbf{d}_k\|)^2 = N(\beta_{1k}^2 + \beta_{2k}^2)$  represents  $k$ th source power on the antenna.

In order to understand the statistical meaning of QSM, the links between quaternions and complex numbers statistics must be studied. Therefore, the output of the vector-sensor array  $\mathbf{x} \in \mathbb{H}^N$  can be written according to the complex-valued outputs  $\mathbf{x}_1, \mathbf{x}_2 \in \mathbb{C}^N$  of the two components of the array as

$$\mathbf{x} = \mathbf{x}_1 + i\mathbf{x}_2. \quad (23)$$

<sup>3</sup>The norm of a quaternion vector  $q$  is defined as  $\|q\| = \sqrt{q^\triangleleft q}$ , where  $\triangleleft$  represents the quaternionic transposition-conjugation operator.

The transpose-conjugate of the quaternion vector  $\mathbf{x}$  can be expressed using transpose-conjugates of the complex vectors  $\mathbf{x}_1, \mathbf{x}_2$  as

$$\mathbf{x}^\triangleleft = \mathbf{x}_1^H - \mathbf{x}_2^H \mathbf{i} \quad (24)$$

with  $H$  the complex transposition-conjugation operator.

Substituting (23) and (24) in (19), the representation of  $\mathbf{\Omega}$  becomes

$$\mathbf{\Omega} = \mathbb{E} \{ \mathbf{x}_1 \mathbf{x}_1^H \} - \mathbb{E} \{ \mathbf{x}_1 \mathbf{x}_2^H \} \mathbf{i} + \mathbf{i} \mathbb{E} \{ \mathbf{x}_2 \mathbf{x}_1^H \} - \mathbb{E} \{ \mathbf{x}_2 \mathbf{x}_2^H \} \mathbf{i}. \quad (25)$$

When considering (25), the reader must keep in mind that  $\mathbf{x}_1, \mathbf{x}_2$  are  $\mathbf{j}$ -complex vectors and multiplication by  $\mathbf{i}$  of a  $\mathbf{j}$ -complex number is not commutative. One can identify in (25) the expressions of auto-covariance and cross-covariance matrices for the two components of the vector array, meaning that QSM contains intrinsically all the second-order information available on the antenna. The fact that none of these matrices is explicitly calculated when estimating QSM reduces the computational time of the algorithm and saves memory.

*Property:* The noise-free part of QSM  $\mathbf{\Omega}_S$  is a Toeplitz matrix.

*Proof:* Consider the signal part of  $\mathbf{\Omega}$

$$\mathbf{\Omega}_S = \sum_{k=1}^K \sigma_k^2 \mathbf{c}_k \mathbf{c}_k^\triangleleft \quad (26)$$

where  $\mathbf{c}_k$  is given by (16). Thus, introducing (16) in (26) and using quaternion product conjugate expression

$$\begin{aligned} \mathbf{\Omega}_S &= \sum_{k=1}^K \left( \frac{\sigma_k}{\|\mathbf{d}_k\|} \right)^2 p_k \mathbf{a}_k \mathbf{a}_k^H \bar{p}_k \\ &= \sum_{k=1}^K \left( \frac{\sigma_k}{\|\mathbf{d}_k\|} \right)^2 p_k \mathbf{A}_k \bar{p}_k \end{aligned} \quad (27)$$

in which  $p_k \in \mathbb{H}$  is given by (12) and  $\mathbf{A}_k = \mathbf{a}_k \mathbf{a}_k^H$  is a complex-Hermitian matrix ( $\mathbf{A}_k \in \mathbb{C}^{N \times N}$ ) presenting a Toeplitz form

$$\mathbf{A}_k = \begin{pmatrix} 1 & e^{\mathbf{j}\theta_k} & \dots \\ e^{-\mathbf{j}\theta_k} & 1 & e^{\mathbf{j}\theta_k} \\ \vdots & e^{-\mathbf{j}\theta_k} & \ddots \\ & & & 1 \end{pmatrix}. \quad (28)$$

Multiplication of  $\mathbf{A}_k$  on the left by  $p_k$  and on the right by  $\bar{p}_k$  conserves the Toeplitz structure:  $\mathbf{C}_k = p_k \mathbf{A}_k \bar{p}_k$ . Thus,  $\mathbf{\Omega}_S$  can be written as a weighted sum of quaternion Toeplitz matrices  $\mathbf{\Omega}_S = \sum_{k=1}^K \beta_{1k}^2 \mathbf{C}_k$ . ■

As the noise component of the signal (see (15)) is assumed spatially white and nonpolarized, the noise part of QSM,  $\mathbf{\Omega}_N = \xi \{ \mathbf{nn}^\triangleleft \}$ , is a real diagonal matrix for which the diagonal entries represent the noise power on the  $N$  sensors.

## B. Subspace Method

Eigenstructure methods are based on the decomposition of the vector space spanned by the observation vector  $\mathbf{x}$  in orthogonal subspaces using an energy criteria.

1) *Quaternion Eigenvalue Decomposition:* Researchers in areas such as quantum mechanics [32], vector-signal processing

[11], [12], and color image processing [33] took interest recently in computation of eigenvalue decomposition (EVD) and the singular value decomposition (SVD) of quaternion matrices. Due to the noncommutativity of quaternions, there are two types (*right* and *left*) of quaternion eigenvalues. Theory about the right quaternionic eigenvalues is well established [28], [34]. However, this is not the case for the left eigenvalues of quaternion matrices, as their existence is still problematic [35]. Therefore, in this paper, the terms *quaternion eigenvalues* and *quaternion eigenvectors* are used for *right eigenvalues* and *right eigenvectors*.

In practice, we have only access to an estimation of the quaternion spectral matrix  $\hat{\mathbf{\Omega}}$  (obtained by classical statistical average or some other averaging technique). By construction, QSM is quaternion Hermitian  $\hat{\mathbf{\Omega}}^\triangleleft = \hat{\mathbf{\Omega}}$ . It can be shown that the eigenvalues for a quaternion Hermitian matrix are real-valued (see [36]). Quaternion spectral matrix can thus be written as

$$\hat{\mathbf{\Omega}} = \sum_{k=1}^N \lambda_k \mathbf{u}_k \mathbf{u}_k^\triangleleft \quad (29)$$

where  $\lambda_k$  are the real eigenvalues and  $\mathbf{u}_k$  are the  $N$  orthonormal quaternion-valued eigenvectors.

2) *Quaternion Vectors Orthogonality:* In order to define orthogonality for quaternion-valued vectors, we have to generalize the definition of *scalar product* to the quaternionic case. For two quaternion-valued column vectors  $\mathbf{w}, \mathbf{y} \in \mathbb{H}^N$ , the scalar product is defined as

$$\langle \mathbf{w}, \mathbf{y} \rangle_{\mathbb{H}} = \mathbf{y}^\triangleleft \mathbf{w}. \quad (30)$$

We say that two quaternion vectors are *orthogonal* if their scalar product is null. Thus, the  $\mathbf{u}_k$  vectors in (29) form a quaternionic orthonormal basis in the observation space spanned by  $\mathbf{x}$ . To better understand how quaternionic orthogonality works, consider two quaternion-valued vectors  $\mathbf{w}, \mathbf{y} \in \mathbb{H}^N$ , having Cayley–Dickson representations, such as

$$\begin{cases} \mathbf{w} = \mathbf{w}_1 + \mathbf{i}\mathbf{w}_2 \\ \mathbf{y} = \mathbf{y}_1 + \mathbf{i}\mathbf{y}_2 \end{cases}. \quad (31)$$

In (31),  $\mathbf{w}_1, \mathbf{w}_2, \mathbf{y}_1, \mathbf{y}_2 \in \mathbb{C}^N$  are complex-valued vectors that can be assimilated to the components of a 2C vector-sensor array (see (23)). If the two components are processed separately as scalar data sets (as in the case of MUSIC for scalar-sensor array), the orthogonality relationships for the vectors of the orthogonal basis can be written as

$$\begin{cases} \mathbf{y}_1^H \mathbf{w}_1 = 0 \\ \mathbf{y}_2^H \mathbf{w}_2 = 0 \end{cases}. \quad (32)$$

The classical subspace methods in vector-sensor array processing use *long-vector orthogonality*, which is in fact the orthogonality for the complex vectors  $\tilde{\mathbf{w}}, \tilde{\mathbf{y}} \in \mathbb{C}^{2N}$  obtained by concatenating the two components

$$\tilde{\mathbf{w}} = \begin{bmatrix} \mathbf{w}_1 \\ \mathbf{w}_2 \end{bmatrix} \quad \text{and} \quad \tilde{\mathbf{y}} = \begin{bmatrix} \mathbf{y}_1 \\ \mathbf{y}_2 \end{bmatrix}. \quad (33)$$

In the first case, the quaternionic orthogonality implies  $\langle \mathbf{w}, \mathbf{y} \rangle_{\mathbb{H}} = 0$ , while in the long-vector case, complex vectors orthogonality implies:  $\langle \tilde{\mathbf{w}}, \tilde{\mathbf{y}} \rangle_{\mathbb{C}} = 0$ . From (30) and (31),

orthogonality between the two vectors of quaternions is equivalent to

$$(\mathbf{y}_1^H - \mathbf{y}_2^H \mathbf{i})(\mathbf{w}_1 + \mathbf{i}\mathbf{w}_2) = 0 \quad (34)$$

which leads to the two equalities

$$\mathbf{y}_1^H \mathbf{w}_1 + \mathbf{y}_2^H \mathbf{w}_2 = 0 \quad (35)$$

and

$$\mathbf{y}_1^T \mathbf{w}_2 = \mathbf{y}_2^T \mathbf{w}_1. \quad (36)$$

Similarly, using the long-vector representations (33), complex orthogonality leads to

$$[\mathbf{y}_1^H \mathbf{y}_2^H] \begin{bmatrix} \mathbf{w}_1 \\ \mathbf{w}_2 \end{bmatrix} = 0 \quad (37)$$

which is equivalent to (35).

It must be noticed that quaternion orthogonality induces one more constraint (36) on the relationship between the two components than does the complex orthogonality. The question is whether the second constraint is incompatible with the first one ((35) excludes (36)) or it is trivial ((35) implies (36)). Two numerical examples are given to answer these questions.

*Example 1:* Consider  $\mathbf{w}_1, \mathbf{w}_2, \mathbf{y}_1, \mathbf{y}_2 \in \mathbb{C}^3$  given by

$$\begin{aligned} \mathbf{w}_1 &= \begin{pmatrix} -0.3286 - 0.1998j \\ -0.3090 - 0.2856j \\ -0.3368 - 0.3534j \end{pmatrix} \\ \mathbf{w}_2 &= \begin{pmatrix} -0.3529 - 0.3546j \\ -0.3103 - 0.1448j \\ -0.0791 - 0.2511j \end{pmatrix} \\ \mathbf{y}_1 &= \begin{pmatrix} 0.1232 - 0.2396j \\ 0.0425 - 0.3371j \\ 0.0709 + 0.4814j \end{pmatrix} \\ \mathbf{y}_2 &= \begin{pmatrix} 0.0804 + 0.1064j \\ -0.2400 + 0.3502j \\ 0.0869 - 0.6080j \end{pmatrix}. \end{aligned}$$

For this set of complex vectors, both relations (35) and (36) are fulfilled, proving the existence of *quaternionic orthogonality* and implying the compatibility of the two constraints.

*Example 2:* A second example is considered with the following numerical values:

$$\begin{aligned} \mathbf{w}_1 &= \begin{pmatrix} -0.2918 - 0.2407j \\ -0.2933 - 0.2334j \\ -0.2549 - 0.2104j \end{pmatrix} \\ \mathbf{w}_2 &= \begin{pmatrix} -0.3124 - 0.2973j \\ -0.4091 - 0.3374j \\ -0.3130 - 0.2048j \end{pmatrix} \\ \mathbf{y}_1 &= \begin{pmatrix} 0.3896 + 0.3205j \\ -0.4620 + 0.2509j \\ 0.3200 - 0.2827j \end{pmatrix} \\ \mathbf{y}_2 &= \begin{pmatrix} -0.2953 - 0.1160j \\ -0.0177 + 0.1209j \\ 0.1220 - 0.3954j \end{pmatrix}. \end{aligned}$$

By calculation, it can be shown that in this case (35) is verified while (36) is not, meaning that the second constraint is not trivial. These vectors are *complex orthogonal (long vector)*, but they are not *quaternion orthogonal*.

*Example 3:* We have shown that (35) does not imply (36). In order to prove that the two constraints are completely independent, it is necessary to show that (36) does not imply (35) either. The numerical example presented next illustrates this statement:

$$\begin{aligned} \mathbf{w}_1 &= \begin{pmatrix} -0.2347 + 0.4077j \\ -0.0740 + 0.3935j \\ 0.0759 - 0.1138j \end{pmatrix} \\ \mathbf{w}_2 &= \begin{pmatrix} 0.0289 + 0.2782j \\ -0.5186 + 0.1381j \\ 0.1498 + 0.4593j \end{pmatrix} \\ \mathbf{y}_1 &= \begin{pmatrix} 0.4650 + 0.2144j \\ -0.0899 + 0.1219j \\ -0.5093 - 0.0066j \end{pmatrix} \\ \mathbf{y}_2 &= \begin{pmatrix} 0.0591 + 0.4422j \\ -0.1730 - 0.2840j \\ 0.2118 - 0.3177j \end{pmatrix}. \end{aligned}$$

For  $\mathbf{w}_1, \mathbf{w}_2, \mathbf{y}_1, \mathbf{y}_2$  described above, relation (36) is verified while (35) is not.

These three numerical examples prove that the two conditions imposed on the complex components are compatible and independent. This signifies that quaternion orthogonality is a "stronger" constraint compared with the complex one

$$\langle \mathbf{w}, \mathbf{y} \rangle_{\mathbb{H}} = 0 \Rightarrow \langle \tilde{\mathbf{w}}, \tilde{\mathbf{y}} \rangle_{\mathbb{C}} = 0. \quad (38)$$

The reciprocal expression is not always true.

We show under which conditions long vector orthogonality and quaternion orthogonality are equivalent. Assimilating  $\mathbf{w}_1, \mathbf{w}_2$ , and  $\mathbf{y}_1, \mathbf{y}_2$  to the components of two polarized sources on a 2C sensor array, the following relations can be written:

$$\begin{cases} \mathbf{w}_2 = \mathbf{w}_1 \rho_w e^{j\varphi_w} \\ \mathbf{y}_2 = \mathbf{y}_1 \rho_y e^{j\varphi_y} \end{cases} \quad (39)$$

where  $\rho_w, \varphi_w$  and  $\rho_y, \varphi_y$  are the polarization parameters of the sources (see (12)). Replacing (39) in (36) leads to

$$\mathbf{y}_1^T \mathbf{w}_1 \rho_w e^{j\varphi_w} = \mathbf{y}_1^T \mathbf{w}_1 \rho_y e^{j\varphi_y}. \quad (40)$$

By imposing this relation to be true for any  $\mathbf{w}_1, \mathbf{y}_1 \in \mathbb{C}^N$ , we get  $\rho_w = \rho_y$  and  $\varphi_w = \varphi_y$ , meaning that sources polarizations are identical. Thus, theoretically (if we do not take into account the statistical aspect in the covariance matrix) the vector basis obtained by imposing quaternion orthogonality or long vector orthogonality are identical only if sources contained in the signal part have identical polarizations or if there is only one source present in the signal. Otherwise, these two methods yield different results. Equations (32), (35), and (36), can be rewritten using the complex scalar product as

$$\begin{cases} \langle \mathbf{w}_1, \mathbf{y}_1 \rangle_{\mathbb{C}} = 0 \\ \langle \mathbf{w}_2, \mathbf{y}_2 \rangle_{\mathbb{C}} = 0 \end{cases} \quad (41)$$

$$\langle \mathbf{w}_1, \mathbf{y}_1 \rangle_{\mathbb{C}} = -\langle \mathbf{w}_2, \mathbf{y}_2 \rangle_{\mathbb{C}} \quad (42)$$

$$\langle \mathbf{w}_1, \mathbf{y}_2^* \rangle_{\mathbb{C}} = \langle \mathbf{w}_2, \mathbf{y}_1^* \rangle_{\mathbb{C}} \quad (43)$$

where \* represents the complex conjugate of a vector. Tables I and II summarize the discussion on vector orthogonality in terms of scalar product between the components. Each cell of

TABLE I  
RELATIONSHIPS BETWEEN THE COMPONENTS WHEN  
PROCESSING EACH COMPONENT SEPARATELY

$\langle \cdot, \cdot \rangle$	$\mathbf{y}_1$	$\mathbf{y}_2$
$\mathbf{w}_1$	0	
$\mathbf{w}_2$		0

TABLE II  
RELATIONSHIPS BETWEEN THE COMPONENTS FOR  
LONG VECTOR AND QUATERNION ORTHOGONALITY

$\langle \cdot, \cdot \rangle$	$\mathbf{y}_1$	$\mathbf{y}_2$	$\mathbf{y}_1^*$	$\mathbf{y}_2^*$
$\mathbf{w}_1$	$\Rightarrow$			$\rightarrow$
$\mathbf{w}_2$		$\Leftarrow$	$\rightarrow$	

$\Rightarrow, \Leftarrow$  : long vector orthogonality constraint

$\Rightarrow, \Leftarrow, \rightarrow$  : quaternion vector orthogonality constraint

the tables corresponds to the scalar product of the associated complex vectors.

The identically shaped arrows indicate which scalar products are forced to be equal (in absolute value). The direction of the arrow designates the sign (right arrow for positive and left arrow for negative) of the product in relationship with the corresponding equal quantity. The double arrows represent the long vector constraint and an empty cell indicates that there is no constraint between the considered vectors. When processing one component at a time (Table I), one can see that there are no links between the scalar products of the components. Each couple of components is forced to orthogonality independently, representing two different self-sufficient estimation problems. The long vector orthogonality imposes a constraint between the corresponding components of the vectors (see Table II—the double arrows)  $((\mathbf{w}_1, \mathbf{y}_1)$  and  $(\mathbf{w}_2, \mathbf{y}_2))$  and the quaternion orthogonality restrains even more the freedom of the components forcing an additional cross-component relationship (Table II—the simple arrows).

An evident question arising after this discussion on orthogonality is what would be the effect of this stronger orthogonality constraint on subspace-based algorithms. We show in the next part that for a two-component complex-valued data set, quaternion vector orthogonality provides a more accurate estimation of the signal subspace than the long vector orthogonality constraint.

Consider two square complex-valued matrices  $\mathbf{C}_1, \mathbf{C}_2 \in \mathbb{C}^{20 \times 20}$ , whose entries are generated using a random uniform number generator.  $\mathbf{C}_1$  and  $\mathbf{C}_2$  could be assimilated to data sets (in the frequency domain) recorded on a two-component array of 20 sensors. Starting from these two matrices, we create a *long vector* complex matrix  $\mathbf{C}_{lv} \in \mathbb{C}^{40 \times 20}$  by concatenation of  $\mathbf{C}_1, \mathbf{C}_2$ , as follows:

$$\mathbf{C}_{lv} = \begin{bmatrix} \mathbf{C}_1 \\ \mathbf{C}_2 \end{bmatrix} \quad (44)$$

and a *quaternion* matrix  $\mathbf{C}_q \in \mathbb{H}^{20 \times 20}$  as

$$\mathbf{C}_q = \mathbf{C}_1 + \mathbf{i}\mathbf{C}_2. \quad (45)$$

After performing the SVD of  $\mathbf{C}_{lv}$  and the quaternion singular value decomposition (QSVD) of  $\mathbf{C}_q$ , the matrices can be written as a sum of 20 rank-1 terms

$$\mathbf{C}_{lv} = \sum_{k=1}^{20} \mathbf{u}_k \sigma_k \mathbf{v}_k^H, \quad \text{where } \mathbf{u}_k \in \mathbb{C}^{40}, \quad \mathbf{v}_k \in \mathbb{C}^{20} \quad (46)$$

$$\mathbf{C}_q = \sum_{k=1}^{20} \mathbf{p}_k \delta_k \mathbf{q}_k^{\triangleleft}, \quad \text{where } \mathbf{p}_k, \mathbf{q}_k \in \mathbb{H}^{20}. \quad (47)$$

The  $\mathbf{u}_k$  complex-valued vectors in (46) and the quaternion vectors  $\mathbf{p}_k$  in (47) form a long vector and a quaternion orthogonal basis respectively in the vector space defined by the two components. Rank- $R$  approximations of  $\mathbf{C}_{lv}$  and  $\mathbf{C}_q$  are constructed as

$$\mathbf{C}_{lv}^R = \sum_{k=1}^R \mathbf{u}_k \sigma_k \mathbf{v}_k^H \quad (48)$$

$$\mathbf{C}_q^R = \sum_{k=1}^R \mathbf{p}_k \delta_k \mathbf{q}_k^{\triangleleft} \quad (49)$$

with  $1 \leq R \leq 20$ .

In order to estimate the rank- $R$  approximation error for the long vector and quaternionic decompositions, the two following error functions are computed:

$$E_{lv}(R) = \frac{\|\mathbf{C}_{lv} - \mathbf{C}_{lv}^R\|}{\|\mathbf{C}_1\| + \|\mathbf{C}_2\|} \quad (50)$$

$$E_q(R) = \frac{\|\mathbf{C}_q - \mathbf{C}_q^R\|}{\|\mathbf{C}_1\| + \|\mathbf{C}_2\|} \quad (51)$$

where  $\|\cdot\|$  is the Frobenius norm<sup>4</sup> of a complex or quaternion matrix.

Fig. 2 plots  $E_{lv}$  and  $E_q$  versus the approximation rank  $R$ . These two curves are obtained by averaging the error functions computed for 100 independent realizations of  $\mathbf{C}_1, \mathbf{C}_2$ . One can see that for a rank-1 approximation, the long vector and the quaternion approaches yield the same estimation error. This is a confirmation of the theoretical result (that we saw earlier in this section) stating that in the case of one source present in the signal (or if sources have identical polarizations) the two kinds of orthogonality are equivalent. For all the other ranks, the approximation error obtained using the quaternionic approach is smaller than the long vector one ( $E_q(R) < E_{lv}(R), 1 < R < 20$ ).

In conclusion, we can state that the use of quaternion vector orthogonality to estimate the signal subspace on a two component vector-sensor array improves estimation accuracy, compared to the long vector method. The explanation is that the energy of the signals on a 2C section can be more precisely concentrated on a quaternion vector orthogonal basis than on a long vector one.

<sup>4</sup>The Frobenius norm of a  $M \times N$  matrix  $\mathbf{A}$  is defined as the square root of the sum of the squared norm of its elements  $\|\mathbf{A}\| = \sqrt{\sum_{m=1}^M \sum_{n=1}^N |a_m^n|^2}$ .

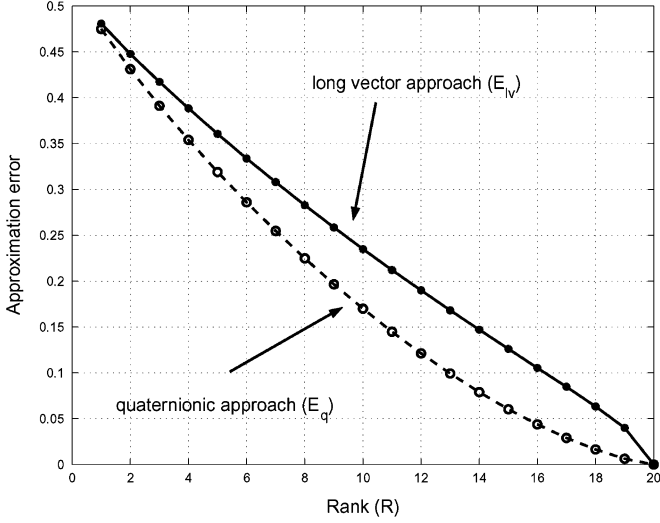


Fig. 2. Rank approximation error for the long vector and quaternionic approaches.

#### IV. QUATERNION-MUSIC ESTIMATOR

Using the data covariance model illustrated in Section III, we propose a MUSIC-like algorithm allowing estimation of DOA (by intersensor phase-shift  $\theta$ ) and polarization parameters  $\rho, \varphi$  (see (16) and (17)). By identification of (21) with (29), we associate the first  $K$  eigenvalues to the signal part of the observation and the rest  $N - K$ , to the noise part. The choice of  $K$  is made by studying the gaps in the quaternionic eigenvalues curve. Statistical criteria such as the Akaike information criterion (AIC) [37] and the minimum description length (MDL) [38] can also be applied, but they are little robust when noise is considered. In the sequel, we consider that  $K$  is *a priori* known and encourage the interested reader to examine the bibliographic references mentioned here.

The quaternion spectral matrix defined in Section III-A can be written in a matrix form as

$$\Omega = \mathbf{C}\Sigma\mathbf{C}^\dagger + \Omega_N \quad (52)$$

with  $\mathbf{C} \in \mathbb{H}^{N \times K}$  containing the  $K$  source vectors  $\mathbf{c}_k(\theta_k, \rho_k, \varphi_k) \in \mathbb{H}^N$  (18) and  $\Sigma \in \mathbb{R}^{K \times K}$  a diagonal matrix containing the sources powers on the antenna,  $\sigma_k^2$ . If noise is not polarized, its covariance matrix is real, diagonal:  $\Omega_N = \sigma_b^2 \mathbf{I}_N$ , where  $\sigma_b^2$  represents noise power on a sensor. Let the EVD of  $\Omega$  be given by

$$\Omega = \mathbf{U}\mathbf{D}\mathbf{U}^\dagger \quad (53)$$

with  $\mathbf{U} = [\mathbf{u}_1, \dots, \mathbf{u}_N] \in \mathbb{H}^{N \times N}$  containing the  $N$  quaternion-valued eigenvectors of  $\Omega$  and  $\mathbf{D} \in \mathbb{R}^{N \times N}$ , the diagonal matrix of its eigenvalues.

We define two matrices  $\mathbf{S} \in \mathbb{H}^{N \times K}$  and  $\mathbf{G} \in \mathbb{H}^{N \times (N-K)}$ , such as

$$\mathbf{S} = [\mathbf{u}_1, \dots, \mathbf{u}_K] \quad (54)$$

$$\mathbf{G} = [\mathbf{u}_{K+1}, \dots, \mathbf{u}_N]. \quad (55)$$

$\mathbf{S}$  contains the eigenvectors corresponding to signal subspace and  $\mathbf{G}$  the eigenvectors corresponding to noise subspace. By multiplying (52) on the right by  $\mathbf{G}$ , we get

$$\Omega\mathbf{G} = \mathbf{C}\Sigma\mathbf{C}^\dagger\mathbf{G} + \sigma_b^2\mathbf{G}. \quad (56)$$

QSM can also be expressed according to  $\mathbf{S}$  et  $\mathbf{G}$  as

$$\Omega = \mathbf{S}\mathbf{D}_S\mathbf{S}^\dagger + \sigma_b^2\mathbf{G}\mathbf{G}^\dagger \quad (57)$$

where  $\mathbf{D}_S = \text{diag}\{\lambda_1, \dots, \lambda_K\}$ . If noise power is equal on all sensors of the array, the last  $N - K$  eigenvalues of  $\Omega$  are all equal to  $\sigma_b^2$ . Replacing (57) in (56), and using the orthogonality between the vectors of  $\mathbf{S}$  and  $\mathbf{P}$ , the following relation is obtained:

$$\sigma_b^2\mathbf{G} = \mathbf{C}\Sigma\mathbf{C}^\dagger\mathbf{G} + \sigma_b^2\mathbf{G} \quad (58)$$

implying

$$\mathbf{C}^\dagger\mathbf{G} = 0. \quad (59)$$

If (59) is multiplied on the right by  $(\mathbf{C}^\dagger\mathbf{G})^\dagger$ , (59) can be expressed using columns of  $\mathbf{C}$  as

$$\mathbf{c}_k^\dagger(\theta_k, \rho_k, \varphi_k)\mathbf{G}\mathbf{G}^\dagger\mathbf{c}_k(\theta_k, \rho_k, \varphi_k) = 0 \quad (60)$$

for all sets of  $\{\theta_k, \rho_k, \varphi_k\}$  corresponding to parameters of  $K$  sources present in the signal.  $\mathbf{\Pi}_N = \mathbf{G}\mathbf{G}^\dagger \in \mathbb{H}^{N \times N}$  represents the *noise subspace projector*. In reality, we only have access to an estimation of this projector,  $\hat{\mathbf{\Pi}}_N$ , resulting from the EVD of the estimated spectral matrix,  $\hat{\Omega}$ .

Quaternion-MUSIC estimator (Q-MUSIC) is then computed by projecting the quaternion steering-vector  $\mathbf{q} \in \mathbb{H}^N$

$$\mathbf{q}(\theta, \rho, \varphi) = \sqrt{N(1 + \rho^2)} \begin{bmatrix} 1 + \mathbf{i}\rho e^{\mathbf{j}\varphi} \\ e^{-\mathbf{j}\theta} + \mathbf{i}\rho e^{\mathbf{j}(\varphi - \theta)} \\ \vdots \\ e^{-\mathbf{j}(N-1)\theta} + \mathbf{i}\rho e^{\mathbf{j}(\varphi - (N-1)\theta)} \end{bmatrix}. \quad (61)$$

on the noise subspace as:

$$M_Q(\theta, \rho, \varphi) = \frac{1}{\mathbf{q}^\dagger(\theta, \rho, \varphi)\hat{\mathbf{\Pi}}_N\mathbf{q}(\theta, \rho, \varphi)}. \quad (62)$$

We find this way, an expression for Q-MUSIC estimator similar to the well-known form of MUSIC algorithm for scalar-sensor array. The functional in (62) has maxima for sets of  $(\theta, \rho, \varphi)$  corresponding to sources present in the signal. By varying  $\theta, \rho, \varphi$  within a given domain with a chosen step, a three-dimensional (3-D) surface is computed. The estimated values of  $\theta, \rho$ , and  $\varphi$  are the coordinates of the most important local maxima on this surface. Assuming that the iteration step is sufficiently small for a correct sampling of the hypersurface, the search for local maxima is automatically done by comparing each point on this surface with its neighbors. The first  $K$  maxima correspond to the  $K$  sources present in the signal.

TABLE III  
COMPUTATIONAL EFFORT FOR COVARIANCE MATRIX ESTIMATION

	Memory requirements ( <i>real values</i> )	Memory operations	Real multiplications (M)	Real additions (A)	Real divisions (D)
QSM	$4N^2$	$\approx 4N^2\Lambda$	$16N^2\Lambda$	$16N^2\Lambda - 4N^2$	$4N^2$
Long-vector SM	$8N^2$	$\approx 8N^2\Lambda$	$16N^2\Lambda$	$16N^2\Lambda - 8N^2$	$8N^2$

This way, the estimation process of  $\theta$ ,  $\rho$ , and  $\varphi$  is quasi-unsupervised.

## V. COMPUTATIONAL ISSUES

This section addresses the problem of computational complexity for long-vector and quaternion algorithms. A full estimation of the computational complexity of the methods is difficult and is little relevant as it is hardware and software dependent. In the sequel we only focus on one aspect of the algorithm: the estimation of the covariance matrix. This procedure, as it implies repetitive operations, best illustrates the complexity difference between the two algorithms. The complexity of the methods are evaluated in terms of memory requirements, memory traffic and basic arithmetical operations: real numbers addition (A), multiplication (M), and division (D).

Let us consider a vector-sensor array composed of  $N$  two-component sensors. In frequency domain, a snapshot of the array is given by two complex-valued vectors  $\mathbf{w}_1, \mathbf{w}_2 \in \mathbb{C}^N$ . The quaternion representation  $\mathbf{w} \in \mathbb{H}^N$  and the long-vector representation  $\tilde{\mathbf{w}} \in \mathbb{C}^{2N}$  of the observation vector have the expressions given by (31) and (33). The corresponding covariance matrices are as it follows:  $\mathbf{\Omega} = \mathbb{E}\{\mathbf{w}\mathbf{w}^{\dagger}\} \in \mathbb{H}^{N \times N}$  and  $\tilde{\mathbf{\Omega}} = \mathbb{E}\{\tilde{\mathbf{w}}\tilde{\mathbf{w}}^H\} \in \mathbb{C}^{2N \times 2N}$ . If averaging over  $\Lambda$  particular realizations of the covariance matrix is used for estimation, we can write  $\mathbf{\Omega} = (1/\Lambda) \sum_{\lambda=1}^{\Lambda} \mathbf{w}_{\lambda}\mathbf{w}_{\lambda}^{\dagger} = (1/\Lambda) \sum_{\lambda=1}^{\Lambda} \mathbf{\Omega}_{\lambda}$  and  $\tilde{\mathbf{\Omega}} = (1/\Lambda) \sum_{\lambda=1}^{\Lambda} \tilde{\mathbf{w}}_{\lambda}\tilde{\mathbf{w}}_{\lambda}^H = (1/\Lambda) \sum_{\lambda=1}^{\Lambda} \tilde{\mathbf{\Omega}}_{\lambda}$ . Each one of the  $\mathbf{\Omega}_{\lambda}$  matrices has  $N^2$  quaternionic entries and can be represented at machine memory level on  $4N^2$  real fields, while the  $\tilde{\mathbf{\Omega}}_{\lambda}$  matrices have  $4N^2$  complex entries each, corresponding to  $8N^2$  real values. This way, quaternion algorithm reduces by half the memory requirements for representation of data covariance model, resulting also in a total diminution by a factor of  $\approx 2$  of memory traffic operations (data retrieving and writing) and a proportional gain in speed.

Let us evaluate now the total number of basic arithmetical operations needed for covariance matrix estimation. Each of the quaternion entries of  $\mathbf{\Omega}_{\lambda}$  is the result of the multiplication of two quaternions. Multiplication of two quaternions implies 16 real multiplications (M) and 12 real additions (A), that is a total of  $16N^2$  (M) and  $12N^2$  (A) for the whole matrix. For the complex matrix  $\tilde{\mathbf{\Omega}}_{\lambda}$  we have  $16N^2$  (M) and  $8N^2$  (A). Thus, the summation  $\sum_{\lambda=1}^{\Lambda} \mathbf{\Omega}_{\lambda}$  needs a total of  $16N^2\Lambda$  (M) and  $12N^2\Lambda + (\Lambda - 1)4N^2 = 16N^2\Lambda - 4N^2$  (A) while  $\sum_{\lambda=1}^{\Lambda} \tilde{\mathbf{\Omega}}_{\lambda}$  requires  $16N^2\Lambda$  (M) and  $8N^2\Lambda + (\Lambda - 1)8N^2 = 16N^2\Lambda - 8N^2$  (A). These results take into account the observation vectors multiplications as well as matrices additions. The final division by  $\Lambda$  means another  $4N^2$  real numbers divisions (D) for the quaternion algorithm and  $8N^2$  (D) for the long-vector one. Table III recapitulates the covariance matrix computational effort for the two algorithms.

As we can see in Table III, the quaternion algorithm reduces the memory requirements for data covariance model representation by a factor of two. Consequently, the memory traffic is reduced by approximately the same factor, resulting in an important gain in rapidity, especially for large data size. Regarding the number of elementary operations on real values, the quaternionic approach demands  $4N^2$  additions moreover and  $4N^2$  divisions less than the long-vector method. The computational complexity for division is several times more important than for addition, implying higher computational cost for long-vector.

The computation of the quaternionic eigenvectors of the estimated matrix  $\mathbf{\Omega} \in \mathbb{H}^{N \times N}$  can be performed using algorithms dealing with complex numbers or quaternions. The methods based on complex numbers come down to diagonalizing the complex adjoint matrix of  $\mathbf{\Omega}$ , that is a complex-valued matrix of size  $2N \times 2N$  (see [28] and [34]). In this case, the computational complexity of the eigenvalue decomposition of the quaternionic matrix  $\mathbf{\Omega}$  is equivalent to the decomposition complexity of the complex matrix  $\tilde{\mathbf{\Omega}}$ . The advantage of this approach is the possibility of using complex matrix diagonalization routines already existing in the literature (e.g., LAPACK), that are computationally optimized.

Nevertheless, it was shown (see [39]) that working directly in quaternionic domain improves the convergence speed of the algorithms compared to complex approach. This reinforces the idea that the use of quaternions can enhance the performance of algorithms.

Generally, the use of quaternions in algorithms reduces the computational effort, due to the compact handling of the data.

## VI. SIMULATION RESULTS

The performances of Q-MUSIC estimator are compared to its scalar version [13] and to Vector-MUSIC (V-MUSIC) [24] for vector-sensor array processing. For the multicomponent algorithms (Q-MUSIC and V-MUSIC), 3-D surfaces (functions of parameters  $\theta, \rho, \varphi$ ) are computed. The presented figures are cuts of this hypersurfaces for fixed values of one or two parameters.

First, we consider a scenario with one polarized source impinging on a 2C-sensor array composed of 10 identical equally-spaced sensors. The source has the DOA  $\theta = 0.93$  rad, polarization parameters:  $\rho = 3, \varphi = 0.27$  rad and random initial phase. Gaussian noise has been added to this signal up to a SNR<sup>5</sup> of 0 dB. A computation step of 0.001 rad has been used for  $\theta$  and 0.05 for  $\rho$  and  $\varphi$ .

<sup>5</sup>If  $S_k^c(\nu)$  and  $N_k^c(\nu)$  are the frequency values for the signal and noise part of the signal on the  $k$ th sensor of the  $c$ th component, the SNR for a 2C data set recorded on  $K$  sensors is defined as  $\text{SNR}(\nu_0) = (\sum_{c=1}^2 \sum_{k=1}^K (S_n^k(\nu_0))^2) / (\sum_{c=1}^2 \sum_{k=1}^K (N_n^k(\nu_0))^2)$  for the working frequency  $\nu_0$ .

In Fig. 3, we have represented the DOA (intersensors phase shift) estimation for the proposed algorithm compared to V-MUSIC and its scalar version, in three different runs for different numbers of snapshots. The curves have been plotted for  $\rho = 3$  and  $\varphi = 0.27$  rad (the polarization parameters of the source). The performance of the new algorithm is comparable to Vector-MUSIC as one can see in Fig. 3(a)–(c). For a large number of samples (a good covariance estimation) [Fig. 3(a)], the 3-dB detection lobe width for Q-MUSIC is even narrower compared with the other vectorial algorithm. This means that for an accurate estimation of QSM, the quaternion algorithm yields better resolution power than V-MUSIC. Fig. 3 shows also that multicomponent information improves considerably the detection resolution; for a poor number of samples scalar detection fails badly [Fig. 3(c)]. Fig. 4(a) and (b) plots the detection curves for polarization parameters ( $\rho$  and  $\varphi$ ) computed by the multicomponent algorithms. This time, a computation step of 0.02 was used for  $\rho$  and  $\varphi$  in order to improve resolution.

Fig. 4(a) and (b) also shows that for a one source scenario, the Q-MUSIC estimation of polarization parameters is equivalent (and sometimes even more performant) to Vector-MUSIC algorithm.

Next, we study the case of two equally powered sources, under the same assumptions. The simulated parameters for the impinging waves are  $\theta_1 = 0.48$  rad,  $\rho_1 = 2.5$ ,  $\varphi_1 = -0.18$  rad, and  $\theta_2 = -0.25$  rad,  $\rho_2 = 3$ ,  $\varphi_2 = 0.15$  rad. In Fig. 5(a), the values of the two three-parameter surfaces, Q-MUSIC and V-MUSIC, are plotted for two fixed values corresponding to polarization parameters of the first source ( $\rho_1 = 2.5$ ,  $\varphi_1 = -0.18$  rad). One can observe that both algorithms present an expected strong answer for the DOA of the first source ( $\theta_1 = 0.48$  rad) and a residual answer for  $\theta_2 = -0.25$  rad corresponding to second source. This residual answer is due to incomplete decorrelation of the two sources. The main detection lobes for Q-MUSIC and V-MUSIC are completely superposed, while the secondary one is slightly stronger for the quaternion method. The explanation is the reduction of data covariance space dimension for Q-MUSIC algorithm (see Section I), resulting in a more important sensitivity of the algorithm to sources correlation. The same phenomenon can be observed for the second source [Fig. 5(b)]; this time, the curves were plotted for two fixed values corresponding to second source polarization parameters.

The polarization parameters plan corresponding to the first source ( $\theta_1 = 0.48$  rad) is represented for Vector-MUSIC estimator in Fig. 6(a) and for Q-MUSIC in Fig. 6(b). In the studied case, both algorithms perform a correct detection; the difference is that detection lobe (cone) is slightly wider for the quaternionic version of the method [Fig. 6(b)] compared with Vector-MUSIC. The situation is similar for the second source polarization parameters. This widening in the polarization domain can be explained by the fact that data covariance compression is performed along the polarization dimension of the data set.

Thus, even in a multiple emitter scenario, the proposed algorithm yields performances comparable to similar techniques (Vector-MUSIC), using less computational resources.

In order to have a statistical characterization of Q-MUSIC estimator, its performance is compared to Vector-MUSIC

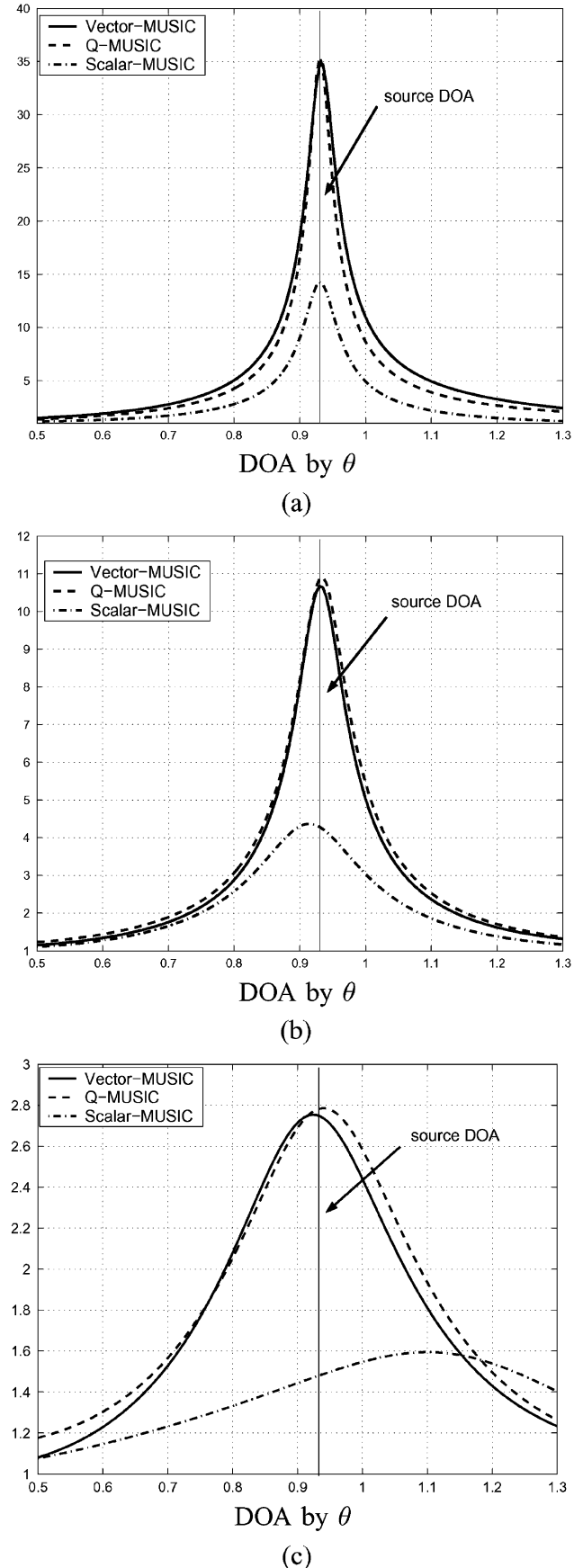
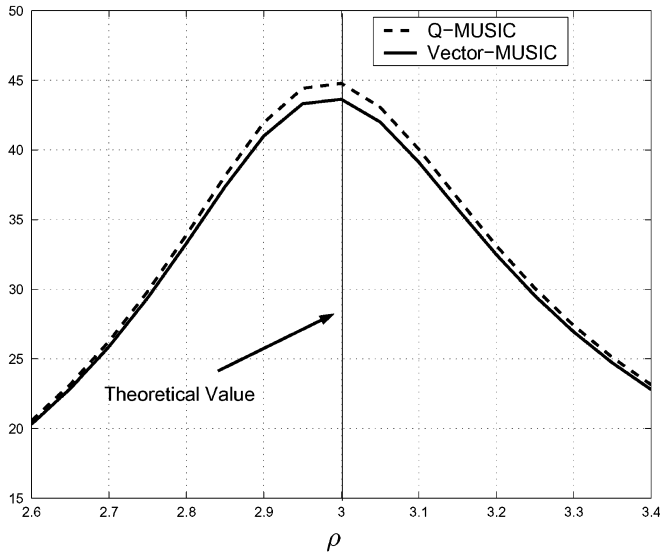
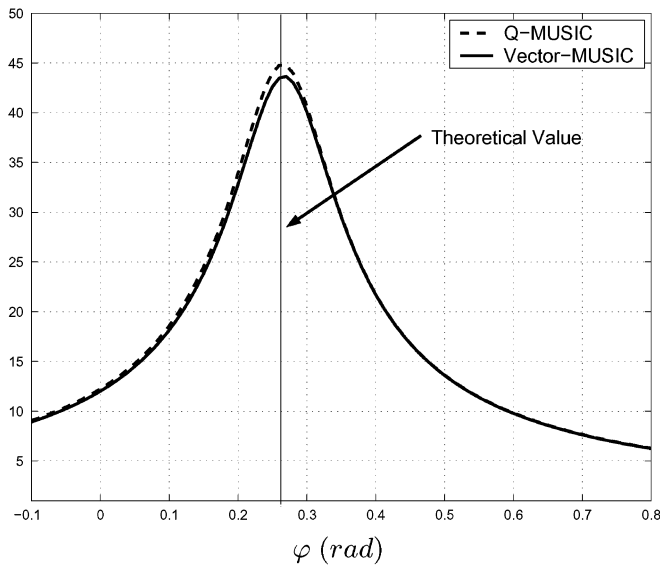


Fig. 3. Q-MUSIC, Vector-MUSIC and Scalar-MUSIC in three runs for different numbers of samples: (a) 1000 ; (b) 100; and (c) 10.



(for  $\theta = 0.93$  rad and  $\varphi = 0.27$  rad)

(a)

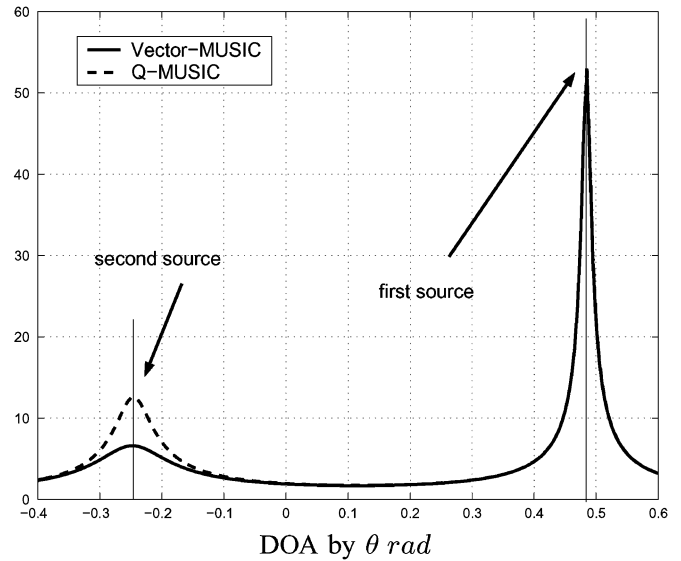


(for  $\theta = 0.93$  rad and  $\rho = 3$ )

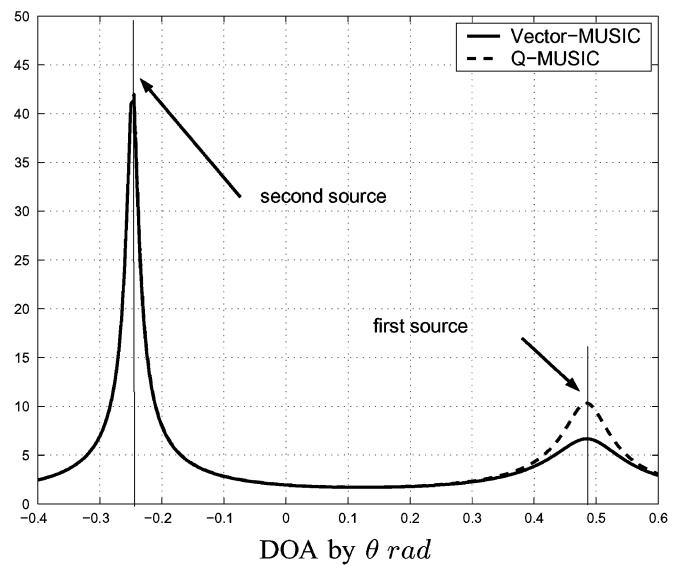
(b)

Fig. 4. Q-MUSIC and Vector-MUSIC estimation for (a)  $\rho$  and (b)  $\varphi$  for 1000 snapshots.

and Scalar-MUSIC estimators in Monte Carlo runs. Two equal-power uncorrelated polarized sources, with random initial phases, impinge on a two-component sensor-array composed of ten equally spaced sensors. The sources DOAs are  $\theta_1 = -0.7$  rad,  $\theta_2 = 0.5$  rad, and they have the following polarization parameters:  $\rho_1 = 2.5$ ,  $\varphi_1 = -0.18$  rad, and  $\rho_2 = 3$ ,  $\varphi_2 = 0.15$  rad. Fig. 7 plots the DOA root-mean-square (rms) estimation error for the estimators mentioned below. One hundred snapshots are used in each Monte Carlo run. Three hundred independent runs contribute to each number in the figure. Additive white Gaussian noise is present in different signal to noise proportions. The rms error of  $\hat{\theta}$  is defined as the rms of the rms estimation error of  $\hat{\theta}_1$  and  $\hat{\theta}_2$  ( $\text{rms}(\hat{\theta}) = \sqrt{(\text{rms}^2(\hat{\theta}_1) + \text{rms}^2(\hat{\theta}_2))/2}$ ). For Scalar-MUSIC, a mean is operated over the two components.



(a)



(b)

Fig. 5. DOA estimation using Q-MUSIC and Vector-MUSIC: (a) Cut for  $\rho_1 = 2.5$ ,  $\varphi_1 = -0.18$  rad (source 1) and (b) cut for  $\rho_2 = 3$ ,  $\varphi_2 = 0.15$  rad (source 2).

Fig. 7 shows that the two algorithms, Q-MUSIC and V-MUSIC, present equivalent performance, their rms error curves are almost totally superposed. Nevertheless, their estimation error is clearly inferior to scalar version of the algorithm.

## VII. CONCLUSION

In this paper, we have illustrated a compact and elegant way of dealing with two-component complex-valued data sets in vector-sensor array processing, using quaternions. A new data model and data covariance model (QSM) was proposed and a new direction-finding method (Q-MUSIC) exploiting spatial and polarization diversity was introduced. This algorithm allows DOA and polarization estimation for multiple sources on a vector-sensor array.

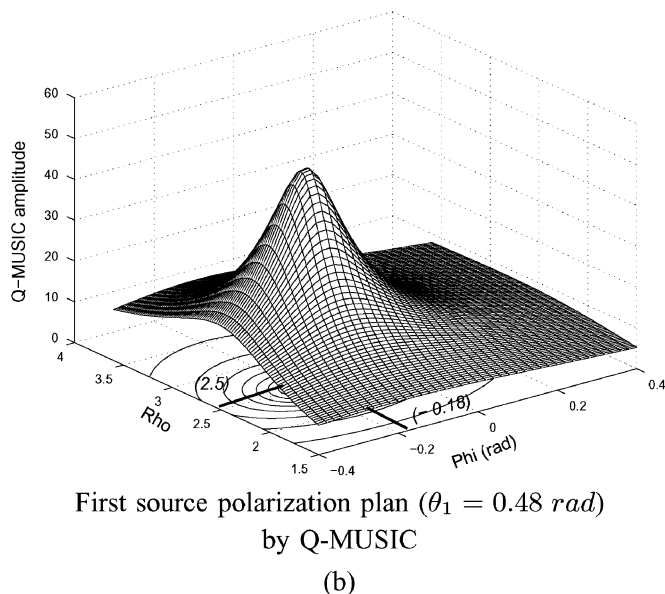
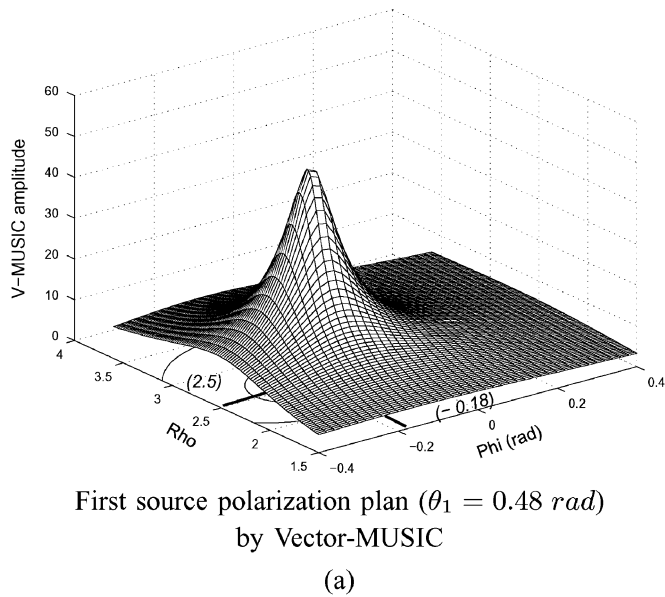


Fig. 6. Polarization estimation for the first source using (a) Vector-MUSIC and (b) Q-MUSIC.

We showed that the quaternion vector orthogonality allows a more accurate estimation of the noise subspace for a two-component data set, compensating for the loss of performance due to the reduction of data covariance representation (QSM) size.

The proposed method has been compared to the classical MUSIC algorithm for scalar-sensor array and to another MUSIC-like algorithm for vector-sensor array processing. Q-MUSIC is clearly more accurate than classical (scalar) MUSIC and yields equivalent results compared with the Vector-MUSIC algorithm, reducing the computational burden and dividing by half the memory space required. The method has a better resolution power for an accurate estimation of the QSM, but it is more sensitive to sources correlation than Vector-MUSIC algorithm. An extended analysis of Q-MUSIC behavior (Cramer–Rao bound, robustness to colored or correlated noise, etc.) is beyond the scope of this paper and should be included in a subsequent paper.

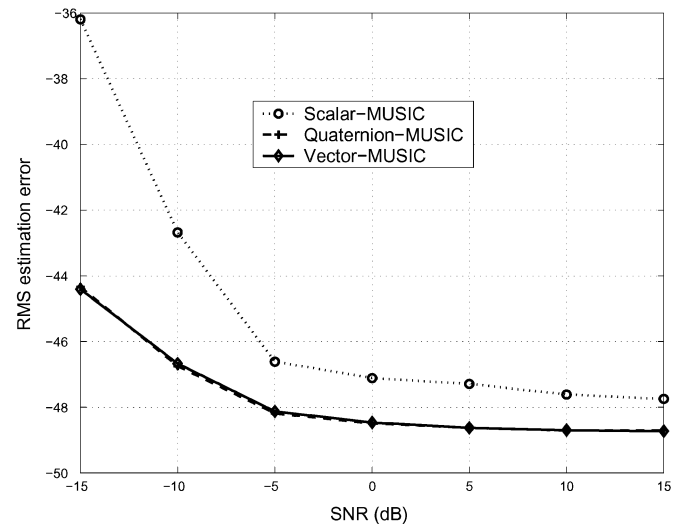


Fig. 7. RMS estimation error (in decibels) for  $\hat{\theta}$  versus SNR (in decibels).

The presented results emphasize the potential of quaternions to model polarized signals and put into perspective the possibility of describing signals having more than two complex-valued components using higher dimensional hypercomplex algebras.

## REFERENCES

- [1] H. D. Schütte and J. Wenzel, "Hypercomplex numbers in digital signal processing," in *Proc. IEEE Int. Symp. Circuits Systems*, 1990, pp. 1557–1560.
- [2] T. A. Ell, "Hypercomplex spectral transformation," Ph.D. dissertation, Univ. of Minnesota, 1992.
- [3] S. J. Sangwine, "Fourier transforms of color images using quaternions, or hypercomplex numbers," *Electron. Lett.*, vol. 32, no. 21, pp. 1979–1980, 1996.
- [4] S. J. Sangwine and T. A. Ell, "The discrete fourier transform of a color image," in *Proc. 2nd IMA Conf. Image Processing*, Leicester, U.K., 1998, pp. 430–441.
- [5] —, "Hypercomplex auto- and cross-correlation of color images," in *Proc. IEEE Int. Conf. Image Processing (ICIP)*, Kobe, Japan, 1999, pp. 319–322.
- [6] S. C. Pei and C. M. Cheng, "A novel block truncation coding of color images using a quaternion-moment-preserving principle," *IEEE Trans. Commun. Syst.*, vol. 45, no. 5, pp. 583–595, May 1997.
- [7] S. L. Hahn, "Multidimensional complex signals with single-orthant spectra," *Proc. IEEE*, vol. 80, pp. 1287–1300, Aug. 1992.
- [8] T. Bülow and G. Sommer, "Hypercomplex signals—A novel extension of the analytic signal to the multidimensional case," *IEEE Trans. Signal Process.*, vol. 49, no. 11, pp. 2844–2852, Nov. 2001.
- [9] N. Le Bihan and J. Mars, "New 2-D complex and hypercomplex attributes," presented at the 71st Conf. Soc. Exploration Geophysicists (SEG), San Antonio, TX, Sep. 2001.
- [10] S. Miron, M. Guillon, N. Le Bihan, and J. Mars, "Multidimensional signal processing using quaternions," in *Proc. 3rd Workshop on Physics Signal Image Processing*, Grenoble, France, Jan. 2003, pp. 57–60.
- [11] N. Le Bihan and J. Mars, "Subspace method for vector-sensor wave separation based on quaternion algebra," presented at the XI Eur. Signal Processing Conf. (EUSIPCO), Toulouse, France, Sep. 2002.
- [12] —, "Singular value decomposition of matrices of quaternions: A new tool for vector-sensor signal processing," *Signal Process.*, vol. 84, no. 7, pp. 1177–1199, 2004.
- [13] R. O. Schmidt, "Multiple emitter location and signal parameter estimation," *IEEE Trans. Antennas Propag.*, vol. 34, no. 3, pp. 276–280, Mar. 1986.
- [14] H. Krim and M. Viberg, "Two decades of array signal processing research: The parametric approach," *IEEE Signal Process. Mag.*, vol. 13, no. 4, pp. 67–94, Jul. 1996.

- [15] L. C. Godara, "Application of antenna arrays to mobile communications—Part I: Performance improvement, feasibility and system considerations," *Proc. IEEE*, vol. 85, pp. 1031–1060, Jul. 1997.
- [16] —, "Application of antenna arrays to mobile communications—Part II: Beam-forming and direction-of-arrival considerations," *Proc. IEEE*, vol. 85, pp. 1195–1245, Aug. 1997.
- [17] K. T. Wong and M. D. Zoltowski, "Self-initiating MUSIC direction finding and polarization estimation in spatio-polarizational beamspace," *IEEE Trans. Antennas Propag.*, vol. 48, no. 9, pp. 1235–1245, Sep. 2000.
- [18] —, "Diversely polarized root-MUSIC for azimuth-elevation angle of arrival estimation," in *Dig. 1996 IEEE Antennas Propagation Soc. Int. Symp.*, Baltimore, MD, Jul. 1996, pp. 1352–1355.
- [19] M. D. Zoltowski and K. T. Wong, "ESPRIT-based 2-D direction finding with a sparse array of electromagnetic vector-sensors," *IEEE Trans. Signal Process.*, vol. 48, no. 8, pp. 2195–2204, Aug. 2000.
- [20] K. T. Wong and M. D. Zoltowski, "Uni-vector-sensor ESPRIT for multi-source azimuth, elevation and polarization estimation," *IEEE Trans. Antennas Propag.*, vol. 45, no. 10, pp. 1467–1474, Oct. 1997.
- [21] J. Li and J. R. Compton, "Angle and polarization estimation using ESPRIT with a polarization sensitive array," *IEEE Trans. Antennas Propag.*, vol. 39, no. 9, pp. 1376–1383, Sep. 1991.
- [22] A. J. Weiss and B. Friedlander, "Performance analysis of diversely polarized antennae arrays," *IEEE Trans. Signal Process.*, vol. 39, no. 7, pp. 1589–1603, Jul. 1991.
- [23] A. Nehorai and E. Paldi, "Vector-sensor array processing for electromagnetic source localization," *IEEE Trans. Signal Process.*, vol. 42, no. 2, pp. 376–398, Feb. 1994.
- [24] S. Miron, N. Le Bihan, and J. Mars, "Vector-MUSIC for polarized seismic sources localization," *EURASIP J. Appl. Signal Process.*, vol. 2005, pp. 74–84, Jan. 2005.
- [25] W. R. Hamilton, "On quaternions," in *Proc. Royal Irish Academy*, 1843.
- [26] I. Kantor and A. Solodovnikov, *Hypercomplex numbers, an elementary introduction to algebras*. New York: Springer-Verlag, 1989.
- [27] J. P. Ward, *Quaternions and Cayley Numbers, Algebra and Applications*. Norwell, MA: Kluwer, 1997.
- [28] H. C. Lee, "Eigenvalues and canonical forms of matrices with quaternion coefficients," in *Proc. Royal Irish Academy*, vol. 52, Dec. 1949, pp. 253–261.
- [29] S. Anderson and A. Nehorai, "Analysis of a polarized seismic wave model," *IEEE Trans. Signal Process.*, vol. 44, no. 2, pp. 379–386, Feb. 1996.
- [30] G. Bienvenu and L. Kopp, "Principe de la goniométrie passive adaptative," *GRETSI*, pp. 106/1–106/10, 1979. in French.
- [31] J. Munier and G. Y. Delisle, "Spatial analysis using new properties of the cross-spectral matrix," *IEEE Trans. Signal Process.*, vol. 39, no. 3, pp. 746–749, Mar. 1991.
- [32] S. De Leo, G. Sclarici, and L. Solombrino, "Quaternionic eigenvalue problem," *J. Math. Phys.*, vol. 43, pp. 5815–5829, 2002.
- [33] N. Le Bihan and S. J. Sangwine, "Quaternion principal component analysis of color images," in *IEEE Int. Conf. Image Process. (ICIP)*, vol. 1, Sep. 2003, pp. 809–812.
- [34] R. M. W. Wood, "Quaternionic eigenvalues," *Bull. London Math. Soc.*, vol. 17, pp. 137–138, 1985.
- [35] L. Huang and W. So, "On left eigenvalues of a quaternionic matrix," *Linear Algebra Its Appl.*, vol. 323, pp. 105–116, 2001.
- [36] F. Zhang, "Quaternions and matrices of quaternions," *Linear Algebra Its Appl.*, vol. 251, pp. 21–57, 1997.
- [37] H. Akaike, "A new look at the statistical model identification," *IEEE Trans. Autom. Control*, vol. 19, no. 6, pp. 716–723, Dec. 1974.
- [38] J. Rissanen, "Modeling by shortest data description," *Automatica*, vol. 14, pp. 465–471, 1978.

- [39] A. Bunse-Gerstner, R. Byers, and V. Mehrmann, "A quaternion QR algorithm," *Numer. Math.*, vol. 55, pp. 83–95, 1989.



**Sebastian Miron** was born in Suceava, Romania, in 1977. He graduated from "Gh. Asachi" Technical University of Iasi, Romania, in 2001 and received the M.Sc. and Ph.D. degree in signal, image, and speech processing from the Institut National Polytechnique of Grenoble, France, in 2002 and 2005, respectively.

He is currently a Teaching Assistant at the Institut Universitaire de Technologie 1 de Grenoble, France, and he is pursuing research at the Laboratoire des Images et des Signaux, Grenoble, France.

His current research interests include seismic data processing, vector-sensor array processing, multilinear algebra, and hypercomplex numbers.



**Nicolas Le Bihan** was born in Morlaix, Brittany, France, in 1974. He received the B.Sc. degree in theoretical physics from the Université de Bretagne Occidentale (UBO), Brest, France, in 1997 and the M.Sc. and Ph.D. degrees in signal processing from the Institut National Polytechnique de Grenoble (INPG), Grenoble, France, in 1998 and 2001, respectively.

Since 2002, he has been Chargé de Recherche at the Centre National de la Recherche Scientifique (CNRS) and is working with the Laboratoire des Images et des Signaux (UMR 5083), Grenoble, France. His research interests include polarized signal processing, multilinear and geometric algebras techniques for vector signal and image analysis, as well as applications of signal processing in geophysics.



**Jérôme I. Mars** received the M.Sc. degree in geophysics from Joseph Fourier University, Grenoble, France, in 1986 and the Ph.D. degree in signal processing from the Institut National Polytechnique, Grenoble, France, in 1988.

From 1989 to 1992, he was a Postdoctoral Researcher at the Centre des Phénomènes Aléatoires et Géophysiques, Grenoble, France. From 1992 to 1995, he was a Visiting Lecturer and Scientist in the Materials Sciences and Mineral Engineering Department, University of California, Berkeley. He is currently Professor of Signal Processing at the Institut National Polytechnique de Grenoble and is with the Laboratoire des Images et des Signaux, Grenoble, France. His research interests include seismic and acoustic signal processing, wavefield separation methods, time-frequency time-scale characterization, and applied geophysics.

Dr. Mars is a Member of the Society of Exploration Geophysicists (SEG) and the European Association of Geoscientists and Engineers (EAGE).